

Density Functional Theory Study of Cu(532)

Faisal Mehmood, Abdelkader Kara, and Talat S. Rahman

Department of Physics, Kansas State University, Manhattan KS 66506, USA

(Dated: December 2, 2024)

Abstract

Using density functional theory and with the generalized gradient approximation and ultra-soft pseudo-potentials, we calculated the structural relaxations of Cu(532) surface. Using a forty layers slab, we find the relaxation pattern to oscillate dramatically for the first 10 atoms before it decays rapidly in the bulk. The most striking feature is an outward expansion of the relative interlayer separation $\Delta\mathbf{d}_{12}$ reaching 25%. We also find serious discrepancies with relaxation pattern and amplitudes calculated using embedded atom method potentials that may reflect the limitation of these potentials to accurately describe systems with complex geometries.

PACS numbers: 11.30.Rd , 65.40.Gr, 68.35.Ja, 68.35.Md, 68.47.De, 82.45.Jn

Nanoscience is increasingly taking the central stage in all aspects of science. From material science to pharmaceutical research, nanotechnology hold the key to advances. Old problems are now looked at and approached with new ideas and techniques as we advance in the knowledge at the nanometer scale. Chirality in natural biological molecules was seen, as early as the 19th century, as the key feature to important properties. The fact that in nature, most of the chiral molecules exist only in one of the two possible forms or enantiomers, is by itself sufficient to excite scientific curiosity. On the other hand, the artificial chiral molecules exist in both forms and only one is of pharmaceutical use. It is then of great technological importance to design efficient enantio-selectors that will retain only the desired enantiomer. Since the two enantiomers of a chiral molecule have the same base atomic structure, their electronic structure is the same and they only differ in the sequence (clock/counter-clock) in which the atomic structure is formed. It is hence logical to use templates/substrates that are naturally or by design chiral [1][2][3]. Regularly kinked surfaces are inherently chiral, and have recently been recently explored for enantio-selectivity [1][2] but several issues are still unresolved. Studies of chiral metal surfaces of Cu and Pt have also been the subject of recent studies [1][2][4][5]. It appears in *ab initio* calculations of Power and Sholl, that the difference in the energetics between relaxed and un-relaxed chiral surfaces of Pt may be important in the evaluation of the difference in adsorption energies of the two different enantiomers of a chiral molecule. These differences in energies are in the range of a few tenths of a kcal/mol or about a few tens of meV. It is hence important to determine as accurate as possible the optimal structure of these kinked surfaces.

In this paper, we present results of electronic structure calculations of Cu(532). Detailed analysis of the structural changes during the relaxation are analyzed and compared to those resulting from empirical potentials to draw their limitations as one moves towards the study of increasingly complex systems.

The chiral/kinked surface Cu(532) is made from a vicinal surface of Cu(111). The unit cell of this surface consists of 8 atoms (having coordination between 6 and 11) as shown in Fig.1.a Since a kink is at the intersection of three planes, (here (111), (100) and (110)) the arrangement of these three planes around the kink atom classifies the surface as being of the R or the S type (here we follow the notations that has been discussed in details by Power and Sholl [4] and Ahmadi *et al* [6]). In Fig. 1b, we show the labeling of the 8 atoms in the unit cell, with the ninth atom being a neighbor of the kink atom with coordination twelve,

labeled here BNN (bulk nearest neighbor). As we shall see, the BNN plays an important role in determining the characteristics of this system.

Our calculations are based on the density-functional theory in the generalized gradient approximation of Perdew-Burke- Ernzerhof [10]. The one particle Kohn-Sham equations [12] are solved self-consistently using the plane-wave basis set using ultra-soft pseudo-potentials [11]. The plane-wave electronic structure calculation code used here is the PWscf provided in the package ESPRESSO [espresso]. In these calculations, the cutoff for the kinetic energy of the plane-waves was set to 400 eV, which ensures excellent convergence of the results. To determine the lattice constant of Cu, electronic structure calculations were performed using one atom per FCC cell with a $10 \times 10 \times 10$ k -points mesh. The resulting lattice constant was found to be 3.65\AA which is less than 1% higher than the experimental value of 3.615\AA . For Cu(532), we have used a slab containing 40 layers and a $3 \times 4 \times 1$ k -points mesh. The ionic relaxation procedure was repeated until the force acting on each atom was less than 10^{-3} eV/ \AA , which was found to be enough to ensure convergent relaxations and energies. In Table 1, we present our results for the relative change in the interlayer separation from the bulk value, along with those obtained using model potentials as described by embedded atom method, using the parameterizations of Voter-Chen [13] (EAM¹) and Foiles-Baskes-Daw as reported recently by Kara and Rahman [8]. We note from Table 1 that both DFT and EAM based results agree on strong contractions of the interlayer separations $\Delta\mathbf{d}_{12}$, $\Delta\mathbf{d}_{23}$, $\Delta\mathbf{d}_{34}$, and $\Delta\mathbf{d}_{45}$, with the tendency of stronger contractions coming from DFT calculations. For $\Delta\mathbf{d}_{56}$, DFT results show a large contraction of about 15%, when EAM based calculations show a very small expansion. The EAM results find a much larger contraction for $\Delta\mathbf{d}_{67}$ than that from DFT. The two methods differ dramatically when it comes to $\Delta\mathbf{d}_{78}$ and $\Delta\mathbf{d}_{89}$ where the embedded atom results show contractions of about 12 – 13% for both these interlayer separations to be contrasted with the DFT results that show nearly no change for $\Delta\mathbf{d}_{78}$ followed by a large expansion of about 25% for $\Delta\mathbf{d}_{89}$. The EAM results differ also from the DFT ones for $\Delta\mathbf{d}_{10,11}$ where, the former show a larger compression than the latter. To further assess the differences between the EAM and DFT results, we analyze the average nearest neighbor distance (Table 2) and the percentage change in the bond length between atoms in atoms in the first 9 layers (Table 2) as labeled in Fig. 1b. From Table 2, we note that in general, the average nearest neighbor change from the bulk value is different for the two methods. For the kink atom, for example, this value is smaller for DFT calculations

than that calculated using EAM. For the 6th and the 7th atom, this value is larger than that of the bulk in the case of DFT calculations, when it shows a lower value than the bulk in the case of EAM results. The analysis presented in Table 3 is of great importance. The bond length between the kink and the 9th (BNN) atoms was found to contract by 5.8% when using DFT calculations, but this contraction is only 3.5% as calculated using EAM, and Barreteau *et al*, using another empirical many-body potential also found a contraction of 3.7%. The larger contraction of this bond can explain the difference between the calculated and the observed high frequency mode on Cu(532). Electron energy loss spectroscopy experiments found a mode on this surface that was about 6.5 meV above the top of the bulk band, but this value was found to be only 2.8 meV by calculations based on EAM [karexp]. We expect a much stronger compression of the bond length between the kink atom and the BNN to produce a surface mode with a frequency higher than 2.8 meV and close to the experimental value.

In summary, we have determined accurately the relaxed structure of Cu(532) using total energy calculations as described by density functional theory. The interatomic bond was found to be stronger than that resulting from empirical many-body potentials, which will has consequences on the dynamics and thermodynamics of this surface. We also expect empirical many-body potentials to show differences with DFT calculations for systems with complex environments as found in nanoparticles.

This work was supported by the US-DOE under the grant DE-FG03-97ER45650.

-
- [1] D.S. Sholl, A. Asthagiri, and T.D. Power, *J. Phys. Chem. B* **105**, 4771 (2001).
- [2] A.J. Gellman, J.D. Horvath, and M.T. Buelow, *J. Mol. Catal. A:Chem.* **167**, 3 (2001).
- [3] M. Schunack, E. Laegsgaard, I. Stensgaard, I. Johannsen, and F. Besenbacher, *Angew Chem.* **113**, 2693 (2001)
- [4] T.D. Power and D. S. Sholl, *Topics in Catal.* **18**, 201 (2002)
- [5] A. Asthagiri, P.J. Feibelman, and D.S. Sholl, *Topics in Catal.* **18**, 193 (2002).
- [6] A. Ahmadi, G. Attard, J. Feliu, and A. Rodes, *Langmuir* **15**, 2420 (1999).
- [7] M.S. Daw and M.I. Baskes, *Phys. Rev. B* **29**, 6443 (1984); S.M. Foiles, M.I. Baskes, and M.S. Daw, *ibid.* **33**, 7983 (1986); M.S. Daw, S.M. Foiles, and M.I. Baskes, *Mater. Sci. Rep.* **9**, 251

(1993).

- [8] T.S. Rahman, A. Kara and S. Durukanoglu, *J. Phys. Condens. Matter* **15**, S3197 (2003)
- [9] S. Durukanoglu, A. Kara, and T. S. Rahman, *Phys. Rev. B* **55**, 13 894 (1997).
- [10] J. P. Perdew and Y. Wang, *Phys. Rev. B* **45**, 13 244 (1992).
- [11] D. Vanderbilt, *Phys. Rev. B* **41**, 7892 (1990).
- [12] W. Kohn and L. Sham, *Phys Rev.* **140**, A1133 (1965).
- [13] S. P. Chen and A. F. Voter, *Surf. Sci.* 244, L107 (1991).

TABLE I: Comparison of relative (to the bulk) interlayer separations. EAM¹ Voter and Chen parametrization. EAM² Foils, Baskes, and Daw parametrization.

$d_{i,i+1}$	EAM ¹	EAM ²	DFT
$d_{1,2}$	-16.23	-14.05	-17.73
$d_{2,3}$	-15.30	-14.44	-18.86
$d_{3,4}$	-9.81	-9.25	-12.71
$d_{4,5}$	-10.09	-9.96	-15.02
$d_{5,6}$	+1.59	+0.85	-14.98
$d_{6,7}$	-6.53	-7.22	-1.36
$d_{7,8}$	+13.16	+11.90	+1.87
$d_{8,9}$	+11.83	+11.68	+24.97
$d_{9,10}$	-8.30	-7.54	-9.72
$d_{10,11}$	-7.94	-8.33	-2.86
$d_{11,12}$	-4.86	-5.06	-4.74
$d_{12,13}$	+1.01	+1.30	-1.99
$d_{13,14}$	+0.42	+0.69	+0.21
$d_{14,15}$	+1.92	+1.26	-1.14
$d_{15,16}$	+3.75	+4.25	+0.05
$d_{16,17}$	+2.40	+2.17	+1.09
$d_{17,18}$	-3.33	-3.23	-1.84
$d_{18,19}$	-3.19	-3.42	-0.71
$d_{19,20}$	-0.54	-0.63	-1.64
$d_{20,21}$	+1.17	+1.65	-0.68

TABLE II: Coordination and average nearest neighbor distance (d_{nn}) in Å. In the first column, we give the bulk d_{nn} , for comparison.

Layer #	1	2	3	4	5	6	7	8	9
coordination	6	7	8	9	9	10	10	11	12
Av. nnd DFT (2.58)	2.51	2.53	2.55	2.57	2.57	2.59	2.59	2.58	2.57
Av. nnd EAM (2.56)	2.50	2.52	2.54	2.54	2.56	2.55	2.55	2.54	2.54

TABLE III: Relative change in the bond length this work and (EAM²).

Layer #	1	2	3	4	5	6	7	8	9
1	-0.8 (-1.1)	-1.6 (-1.1)	-3.1 (-2.0)			-1.6 (-2.7)		-4.3 (-3.2)	-5.8 (-3.5)
2		+0.4 (-0.2)	-1.6 (-1.3)	-2.3 (-0.6)			-0.8 (-2.7)		-3.1 (-1.7)
3			+0.8 (+0.5)	-0.8 (-0.1)	-0.8 (+0.2)			-0.4 (-1.6)	
4				+0.8 (+0.5)	-0.8 (-0.6)	-1.6 (-0.2)			+2.3 (+0.4)
5					0.0 (-0.3)	0.0 (0.2)	-1.6 (-0.6)		
6							+0.4 (-0.4)	+0.8 (+1.2)	+0.8 (+1.0)
7								-0.8 (-0.7)	+0.4 (+0.6)
8									+2.7 (+0.9)

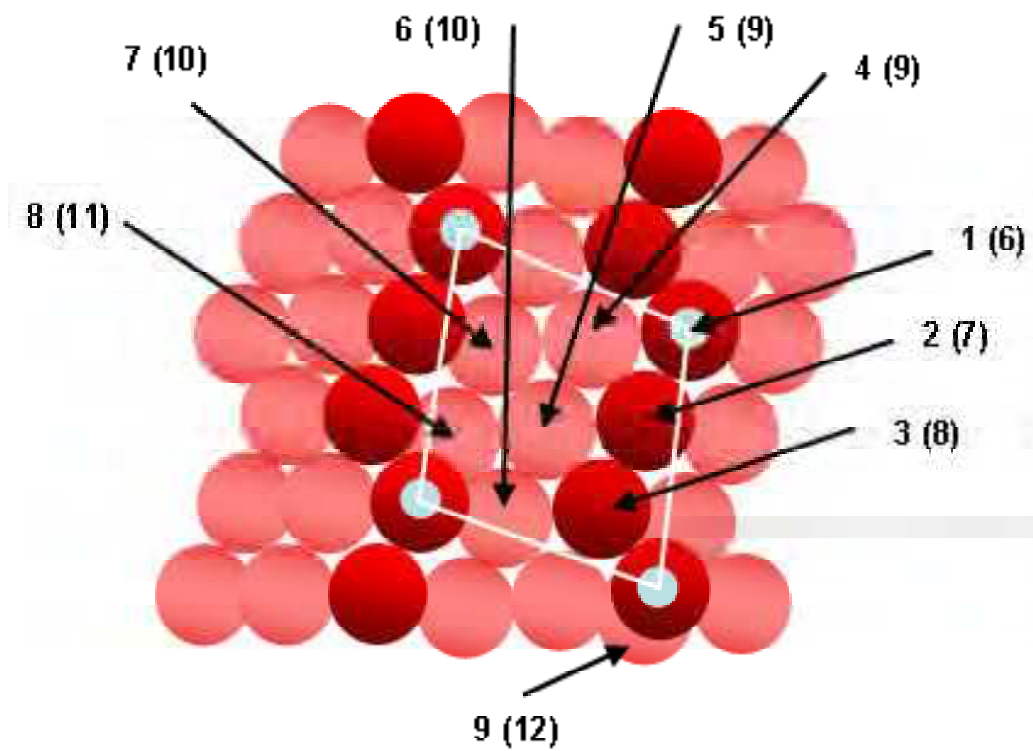
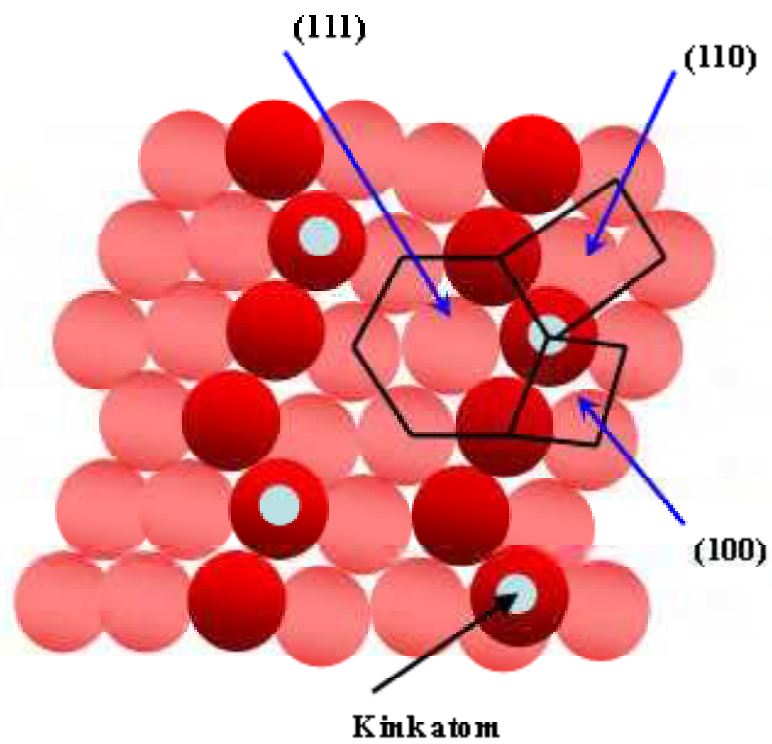


Figure 1: Schematic of fcc(532): a) the unit cell and the different planes forming the kink; b) labeling of the atoms.